International Journal of Innovative Computing, Information and Control
Volume **19**, Number **2**, April **2023**

ICIC International ©2023 ISSN 1349-4198
pp. **549–562**

PRE-SEPARATION TRAJECTORY DESIGN AND CONTROL FOR HORIZONTAL-TAKEOFF REUSABLE LAUNCH VEHICLE

Honglin Liu[1,2,*], Rui Wang[1,2], Weiguang Shao[1,2] and Kai Liu[1,2]

[1]Laboratory of Advanced Technology for Aerospace Vehicles
[2]School of Aeronautics and Astronautics
Dalian University of Technology
No. 2, Linggong Road, Ganjingzi District, Dalian 116024, P. R. China
{ ruiwang; carsonliu }@dlut.edu.cn; 32203116@mail.dlut.edu.cn
*Corresponding author: honglin_liu@mail.dlut.edu.cn

Received July 2022; revised November 2022

Abstract. *Reusable launch vehicles (RLV) are the inevitable trend to achieve fast, reliable, and inexpensive access to space in the future, and are also a current research hotspot in the aerospace field. To address the safety requirements of hypersonic multi-body separation of two-stage-to-orbit (TSTO) RLV, in this paper, a parabolic-shaped ascent trajectory for multi-body separation is designed in terms of safety, and proposes a trajectory profile solution method based on horizontal displacement derivative with known trajectory shape. And then the trajectory linearization control (TLC) method is combined with the solved trajectory profile for the design study of the guidance rate. Finally, the feasibility of the proposed trajectory strategy and the profile solving algorithm is analyzed and verified by simulation in MATLAB, and the tracking control effect of the parabolic separation trajectory designed in this paper is tested.*

Keywords: Reusable launch vehicles (RLV), Pre-separation trajectory design, Multi-body separation, Trajectory linearization control

1. **Introduction.** An RLV is a multipurpose reusable vehicle capable of rapidly traversing the atmosphere and freely traveling. It is a multi-purpose reusable vehicle that can travel rapidly through the atmosphere and freely between the Earth's surface and space. It can deliver payloads to space quickly and conveniently, and can also stay orbit or maneuver for a longer period of time, and then land safely and accurately on the ground after completing its mission. It can land safely and accurately on the ground after completing its mission.

The existing muti-body RLV entering orbit solutions are dominated by single-stage-to-orbit (SSTO) and two-stage-to-orbit (TSTO) solutions. Compared to SSTO solutions, TSTO is more engineering realizable and is the core of current development. The horizontal takeoff TSTO RLV uses a back-loading scheme, i.e., the RLV consists of a carrier and a spacecraft on its back, which is boosted by the carrier's engine during takeoff, takes off horizontally, and then climbs until it reaches the scheduled separation window. During separation, the dorsal vehicle is detached from the carrier by the actuator, and it is pointed out in the work of [1,2] that strong aerodynamic interference between the two vehicles is generated due to the high supersonic speed characteristic of the separation window in general.

Currently, all countries in the world are engaged in fierce competition in the field of aerospace vehicle (ASV) and RLV, in which the United States is in the lead. As researched

DOI: 10.24507/ijicic.19.02.549

in [3-7], the United States has accumulated much experience in RLV multi-body separation through the implementation of projects such as the Quicksat program, Aztec program, and Boeing FASST program. In Europe, the HOTOL program proposed by the UK has made an attempt in the field of air and space flight. The separation mechanism of the Sanger II program proposed by Germany is of great reference value [8], which uses a back-loaded parallel layout that mechanically lifts the upper stage during separation to produce a predetermined angle of attack for safe separation.

In terms of separation trajectory design, there are many kinds of numerical algorithms for trajectory optimization; in general, they are mainly divided into direct and indirect methods. Dalle et al. gave a hypersonic vehicle fixed dynamic pressure climb trajectory design method [9]. Keshmiri et al. established six-DOF dynamics equations for the ascending section of the hypersonic vehicle, and combined the idea of direct method to consider the terminal constraint of the estimated optimization problem, and used the toolkit in MATLAB for trajectory optimization design [10]. Peng et al. [11] gave a method to design the trajectory of the automatic landing section of the carrier based on the geometry of the trajectory profile, combined with the mass point dynamics equation and then the detailed simulation of the trajectory profile; Sun et al. [12] proposed a method to design the trajectory of the ascending section of the hypersonic vehicle based on the preset dynamic pressure. In terms of trajectory tracking guidance, [13] gave a criterion for determining a nonlinear system as a nonminimum phase system for a class of aspirated hypersonic vehicles with nonminimum phase characteristics, and completed a longitudinal trajectory tracking control design using a dynamic inverse method. For the fast time-varying, strong coupling and highly nonlinear characteristics of the longitudinal model of hypersonic vehicle, a Gauss pseudo-spectral approach to the trajectory optimization of the ascending segment is proposed in [14]. According to the thrust characteristics of the engine, the rise trajectory is divided into reasonable segments, and the original optimal control problem is transformed into a multi-segment optimal control problem. After that, the Gauss pseudo-spectral method is used to carry out the parallel optimization calculation. In [15], Kumyaito and Tamee proposed methods to collect, preprocess, and analyze the GPS tracking data from the existing online service for cyclists, and showed that QuickBundles has the capability of clustering the trajectory data in terms of computational speed and validity.

The paper is organized as follows, Section 2 elucidates the mathematical model of the longitudinal dynamics of the RLV and the equations of the trajectory profile based on the horizontal displacement derivative (In the later text, HDD is used instead to indicate horizontal displacement derivative). In Section 3, a trajectory profile solving strategy based on a given shape is proposed. Section 4 presents the TLC tracking design. Section 5 presents the MATLAB simulation results. Section 6 gives conclusion.

2. **The RLV Dynamics Model and HDD Based Trajectory Profile Equations.**

The longitudinal dynamics model of RLV during pre-separating ascent is established in this section. In this paper, ignoring the effect of Earth's auto-transfer and assuming the earth to be flat (ignoring the effect of Earth's radius), the longitudinal dynamics equation of the RLV can be established according to the conversion between the track coordinate system and the ground coordinate system as [16]:

$$\begin{cases} m\dfrac{dV}{dt} = T\cos\alpha - D - mg\sin\theta \\ mV\dfrac{d\theta}{dt} = T\sin\alpha + L - mg\cos\theta \\ \dfrac{dh}{dt} = V\sin\theta \\ \dfrac{dR}{dt} = V\cos\theta \\ \dfrac{dm}{dt} = -\dfrac{T}{I_{sp}g} \end{cases} \tag{1}$$

In the above equation, h, V, θ, m, R indicate altitude, speed, flight path angle, mass and horizontal displacement respectively, T, D, L stand for thrust, drag and lift, I_{sp} stands for engine ratio impulse, and α is angle of attack. The equation for dynamic pressure q is

$$q = \frac{1}{2}\rho V^2 \tag{2}$$

where ρ is atmospheric density.

In this paper, a method of trajectory design based on HDD (horizontal displacement derivative) is proposed for the design of pre-separation ascending trajectories, so that the trajectory of the RLV follows a given shape. The dynamics model based on the HDD is developed for this method and the derivation process is as follows.

Derive the dynamic pressure with respect to time according to the dynamic pressure expression (2), and we have (3).

$$\frac{dq}{dt} = \frac{1}{2}\frac{d\rho}{dR}\frac{dR}{dt}V^2 + \rho V\frac{dV}{dt} \tag{3}$$

Combining (3) with the fourth equation of (1), the derivative of the dynamic pressure with respect to the range is obtained as

$$\frac{dq}{dR} = q\left(\frac{d\rho}{dR}\frac{1}{\rho} - \frac{\rho SC_D}{m\cos\theta}\right) + \frac{\rho T\cos\alpha}{m\cos\theta} - \rho g\tan\theta \tag{4}$$

where C_D is drag factor. This formula represents the rate of change of dynamic pressure about range in the trajectory profile. Then observe the second equation of (1), and move m and V to the right of the equation.

$$\frac{d\theta}{dt} = \frac{1}{V}\left(\frac{T\sin\alpha + L}{m} - g\cos\theta\right) \tag{5}$$

Bringing in the fourth equation of (1), the derivative of the flight path angle with respect to the range is obtained as

$$\frac{d\theta}{dR} = \frac{\rho}{2\cos\theta}\left(\frac{T\sin\alpha}{mq} - \frac{g\cos\theta}{q} + \frac{SC_L}{m}\right) \tag{6}$$

where C_L is lift factor. The equation expresses the rate of change of the flight path angle in the trajectory profile with respect to the range. The third and fourth equations of (1) are quantified to obtain the following equation:

$$\frac{dh}{dR} = \tan\theta \tag{7}$$

Then the third and fifth equations of (1) are quantified to obtain

$$\frac{dm}{dR} = -\frac{T}{gI_{sp}V\cos\theta} \tag{8}$$

Equation (8) then denotes the quality due to fuel consumption as to the rate of change in range.

So far, the HDD based dynamics model of RLV is obtained as Equations (4), (6), (7) and (8). Then Equation (4) is equivalently varied to obtain the trajectory expression for the dynamic pressure:

$$q = \frac{mg\cos\theta - T\sin\alpha}{SC_L - \frac{2m}{\rho}\frac{d\theta}{dR}\cos\theta} \tag{9}$$

The above equation shows the relationship between dynamic pressure and horizontal displacement. This correlation links the dynamic pressure to the trajectory profile, so that the current horizontal displacement can be used to find the dynamic pressure at this time, and conversely the current flight range can be found based on the dynamic pressure at a given moment.

3. **Parabolic Shaped RLV Pre-Separation Trajectory Profile Solving Strategy.**

The normal phase overload of the TSTO RLV at the moment of separation has a great influence on whether it can be separated safely. If the overall overload vector of the RLV is in the same direction as the lift, after separation occurs, the RLV will have a tendency to move upward due to the sudden reduction of spacecraft mass, and at this time the normal phase overload is too large, which will make the carrier move upward and threaten the spacecraft. If the direction of the overload vector is the same as gravity, the spacecraft will not be able to climb upward rapidly, and under the influence of the separation aerodynamic disturbance, the spacecraft will easily lose stability and collide with the carrier.

Given all of the above, this paper proposes a parabolic-shaped ascending trajectory before separation, designs the RLV to have a normal overload of zero at the parabolic apex and executes the separation process of the assembly at the top of the parabola; the trajectory strategy has the following characteristics. 1) At the end of the parabolic trajectory, the flight path angle of the RLV is zero, and the angle of attack is very small, so it is easy to make the combined force of the thrust component in the vertical direction and the lift force zero, so as to achieve the normal overload of zero. 2) The normal overload at the moment of separation is designed to be zero, so that the carrier will not produce an excessive tendency of upward motion after separation, and at the same time the spacecraft is also easy to produce a head-up moment through rudder control, so as to quickly principle the aerodynamic interference area of the carrier and improve the safety of separation. 3) When the vehicle flies according to the parabolic trajectory, the control parameters such as angle of attack and thrust force change smoothly, which reduces the burden on the control system.

First, a mathematical description of the parabolic trajectory is needed. In the design of the parabolic pre-separation ascending trajectory using the method devised in the previous section, a mathematical description is first required, and the relationship between altitude and range is given by

$$h(R) = h_f + a\big(R - R_f\big)^2 \tag{10}$$

where R_f, h_f are the horizontal displacement and altitude of the end-of-trajectory, h_0 is the climb starting height, and a is the parabolic parameter. According to Equation (7), the relationship between flight path angle and range in the longitudinal path can be found as follows:

$$\theta = \arctan\left(\frac{dh}{dR}\right) = \arctan\big(2a\big(R - R_f\big)\big) \tag{11}$$

Letting θ be the derivative for the voyage yields

$$\frac{d\theta}{dR} = \frac{d}{dR}\left[\arctan\left(\frac{dh}{dR}\right)\right] = \frac{1}{1+\left(\frac{dh}{dR}\right)^2}\frac{d^2h}{dR^2} = \frac{2a}{1+4a^2\left(R-R_f\right)^2} \tag{12}$$

This equation describes the relationship between θ and the range in the flight profile of a parabolic trajectory.

After the description of the parabolic ascent trajectory, the trajectory profile strategy is designed. The trajectory profile solving algorithm is shown in Figure 1.

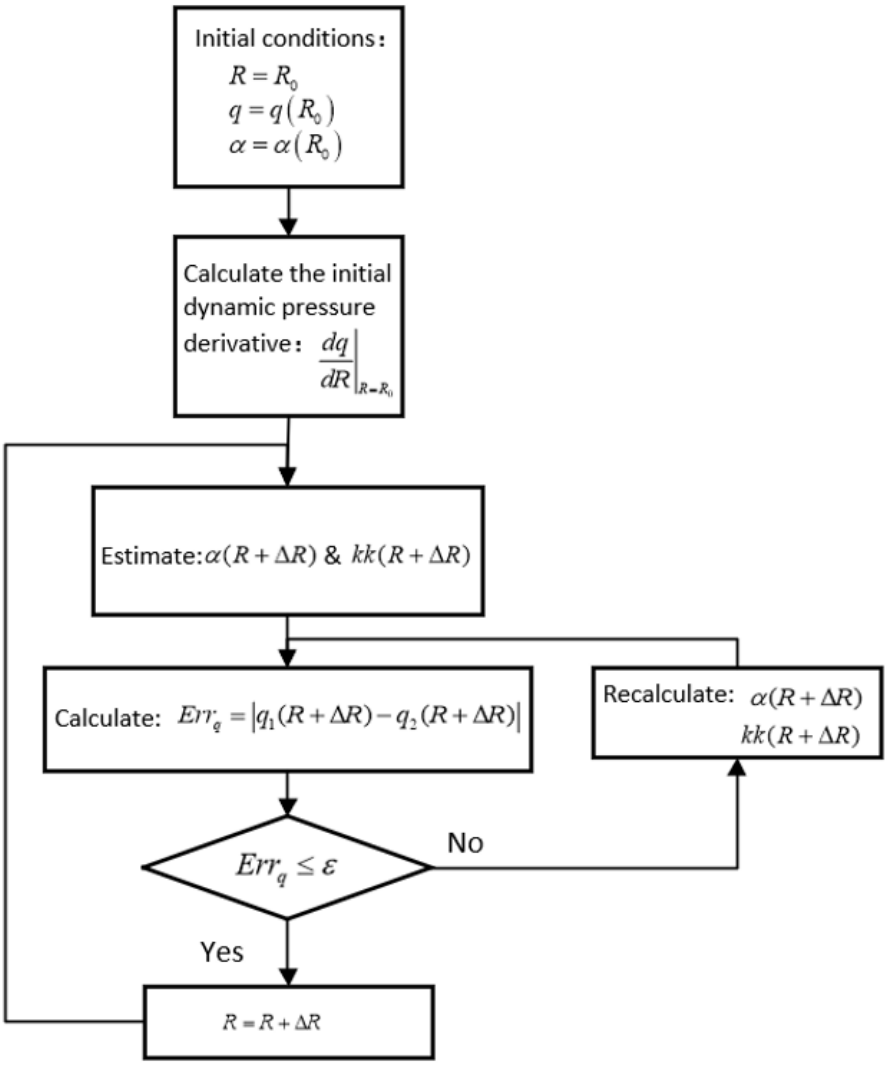

FIGURE 1. The trajectory profile solving algorithm, kk indicates the throttle parameter

As shown in Figure 1, after giving the initial range coordinates, initial dynamic pressure, initial angle of attack and other parameters, the calculation of the initial dynamic pressure about the range change rate is carried out. Then the iterative process begin, and the angle of attack and throttle are estimated separately due to their different physical characteristics. Since $\alpha(R + \Delta R)$ mainly affects the lift of the vehicle, the angle of attack can be estimated from the vehicle normal overload n_y. The n_y is solved in the kinematic model based on the range derivative by

$$n_y = \frac{2q}{\rho g}\frac{d\theta}{dR}\cos\theta + \cos\theta \tag{13}$$

Combined with the normal phase overload equation in the kinetic model, the estimation of $\alpha(R+\Delta R)$ can be derived as follows.

$$\frac{T\sin\alpha+L}{mg}=\frac{2q}{\rho g}\frac{d\theta}{dR}\cos\theta+\cos\theta \tag{14}$$

The same can be derived for the calculation of the estimation of $kk(R+\Delta R)$.

$$\frac{T\cos\alpha-D}{mg}=\frac{V}{g}\frac{dV}{dR}\cos\theta+\sin\theta \tag{15}$$

Once the initial values of $\alpha(R+\Delta R)$ and $kk(R+\Delta R)$ have been estimated, the exact solution under each range needs to be performed, and the value of the $\alpha(R+\Delta R)$ is calculated exactly by means of an optimization algorithm in general. The definition of a function $Q(\alpha,kk)$ is given below.

$$Q(\alpha,T)=q_1(R+\Delta R)-q_2(R+\Delta R) \tag{16}$$

The function $Q(\alpha,kk)$ is mainly used in the Newtonian iterative calculation of $\alpha(R+\Delta R)$. Its physical significance is related to the leveling of the normal overload by $\alpha(R+\Delta R)$. On the one hand, we can use Euler's method to calculate from the first equation of (4) the value of $q(R+\Delta R)$.

$$q_1(R+\Delta R)=q(R)+\frac{\Delta R}{2}\left[\frac{dq}{dR}(R)+\frac{dq}{dR}(R+\Delta R)\right] \tag{17}$$

On the other hand, we can use the data of $\alpha(R+\Delta R)$ by (9) to calculate $q(R+\Delta R)$:

$$q_2(R+\Delta R)=f_2[\alpha(R+\Delta R),R+\Delta R] \tag{18}$$

When the conditions are met:

$$Err_q=|q_1(R+\Delta R)-q_2(R+\Delta R)|\le\varepsilon \tag{19}$$

That is, the iterative computation on this range can be ended and the next range can be computed.

4. **Parabolic Climbing Trajectory TLC Design.** The trajectory linearization control (TLC) technique is a control tool for nonlinear systems, and its control logic is designed by linearizing the nonlinear and time-varying errors between the current flight state and the nominal trajectory state for tracking control law [17], and the parabolic separation trajectory flight profile explored in this paper has the following characteristics [18]: 1) the mass of the vehicle becomes progressively smaller during flight as fuel is consumed, and the center of gravity and rotational inertia change; 2) the core purpose of the pre-separation climb trajectory is to have the normal phase overload of the parallel assemblies be zero at the end of the trajectory, for which the vehicle must strictly control the tracking error in the tracking of velocity, thrust, and flight path angle. This requires a controller with high robustness and good stability within the entire parabolic climb separation trajectory.

In the previous section, the nominal trajectory of the ascent section was obtained by the trajectory design method, and the flight profiles of speed and altitude in each flight process were obtained, and the trajectory tracking control was designed below, and the designed trajectory tracking control block diagram is shown in Figure 2.

We refer to [19-22] to establish the RLV dynamics model. For the height profile and velocity profile tracking needs, the influence of the height/velocity term is taken as the state

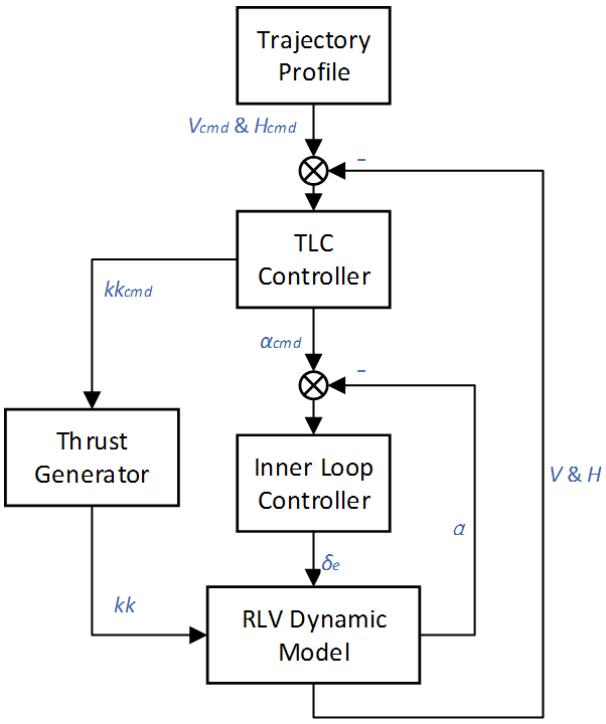

FIGURE 2. Tracking control design

variable of interest, the velocity integral term and the height differential term are introduced to expand the dimensionality of the state equation, and the augmented trajectory dynamics model is as follows.

$$\begin{cases} \dfrac{d\left(\int V dt\right)}{dt} = V \\ \dfrac{dV}{dt} = \dfrac{T\cos\alpha - D}{m} - g\sin\theta \\ \dfrac{dh}{dt} = V\sin\theta \\ \dfrac{d^2h}{dt^2} = \dfrac{T\sin(\theta+\alpha) - D\sin\theta + L\cos\theta - mg}{m} \end{cases} \tag{20}$$

Describing the kinetic model of augmentation as a state space form:

$$\begin{cases} \dot{\boldsymbol{x}}(t) = \boldsymbol{f}(\boldsymbol{x}(t), \boldsymbol{u}(t)) \\ \boldsymbol{x}(t) = \left[\int V(t)dt, V(t), h(t), \dot{h}(t)\right]^{\mathrm{T}} \\ \boldsymbol{u}(t) = [\alpha(t), k_r(t)]^{\mathrm{T}} \end{cases} \tag{21}$$

Defining $\boldsymbol{e} = \boldsymbol{x} - \bar{\boldsymbol{x}}$ and $\bar{\boldsymbol{u}} = \boldsymbol{u} - \tilde{\boldsymbol{u}}$, to describe the error in the actual course of the flight with respect to the deviated trajectory, we have

$$\dot{\boldsymbol{e}}(t) = \boldsymbol{f}(\boldsymbol{x}(t), \boldsymbol{u}(t)) - \boldsymbol{f}(\bar{\boldsymbol{x}}(t), \tilde{\boldsymbol{u}}(t)) \tag{22}$$

Then a linearization along $\boldsymbol{e}(t) = 0$, $\tilde{\boldsymbol{u}}(t) = 0$ yields

$$\dot{\boldsymbol{e}}(t) = \boldsymbol{A}(t)\boldsymbol{e}(t) + \boldsymbol{B}(t)\tilde{\boldsymbol{u}}(t) \tag{23}$$

where

$$\begin{cases} \boldsymbol{A}(t) = \boldsymbol{A}\left(\bar{\boldsymbol{x}}, \bar{\boldsymbol{u}}\right) = \left(\dfrac{\partial \boldsymbol{f}}{\partial \boldsymbol{x}}\right)\Big|_{\bar{\boldsymbol{x}},\bar{\boldsymbol{u}}} = \left[\begin{array}{cccc} 0 & 1 & 0 & 0 \\ 0 & a_{22} & a_{23} & 0 \\ 0 & 0 & 0 & 1 \\ 0 & a_{42} & a_{43} & 0 \end{array}\right]\Bigg|_{\bar{\boldsymbol{x}},\bar{\boldsymbol{u}}} \\ \boldsymbol{B}(t) = \boldsymbol{B}\left(\bar{\boldsymbol{x}}, \bar{\boldsymbol{u}}\right) = \left(\dfrac{\partial \boldsymbol{f}}{\partial \boldsymbol{u}}\right)\Big|_{\bar{\boldsymbol{x}},\bar{\boldsymbol{u}}} = \left[\begin{array}{cc} 0 & 0 \\ b_{21} & b_{22} \\ 0 & 0 \\ b_{41} & b_{42} \end{array}\right]\Bigg|_{\bar{\boldsymbol{x}},\bar{\boldsymbol{u}}} \end{cases} \tag{24}$$

$$\begin{cases} a_{22} = \left(\dfrac{\partial T}{\partial V}\cos\alpha - \dfrac{\partial D}{\partial V}\right)\Big/ m \\ a_{23} = \left(\dfrac{\partial T}{\partial h}\cos\alpha - \dfrac{\partial D}{\partial h}\right)\Big/ m \\ a_{42} = \left[\sin(\theta+\alpha)\dfrac{\partial T}{\partial V} - \sin\theta\dfrac{\partial D}{\partial V} + \cos\theta\dfrac{\partial L}{\partial V}\right]\Big/ m \\ a_{43} = \left[\sin(\theta+\alpha)\dfrac{\partial T}{\partial h} - \sin\theta\dfrac{\partial D}{\partial h} + \cos\theta\dfrac{\partial L}{\partial h}\right]\Big/ m \\ b_{21} = \left(-T\sin\alpha - \dfrac{\partial D}{\partial \alpha}\right)\Big/ m \\ b_{22} = \dfrac{\partial T}{\partial k_r}\cos\alpha\Big/ m \\ b_{41} = \left[\cos(\theta+\alpha)T - \sin\theta\dfrac{\partial D}{\partial \alpha} + \cos\theta\dfrac{\partial L}{\partial \alpha}\right]\Big/ m \\ b_{42} = \sin(\theta+\alpha)\dfrac{\partial T}{\partial k_r}\Big/ m \end{cases} \tag{25}$$

In order to be able to apply the trajectory linearization control method based on the desired pole configuration, the control input matrix is assumed to be non-singular, which is

$$\left|\begin{array}{cc} b_{21} & b_{22} \\ b_{41} & b_{42} \end{array}\right| \neq 0 \tag{26}$$

The time-varying controller design is carried out for the time-varying system after linearization, including the feedforward control part of the nominal trajectory design and the error time-varying feedback controller.

$$\boldsymbol{u}(t) = \bar{\boldsymbol{u}}(t) + \tilde{\boldsymbol{u}}(t) \tag{27}$$

where

$$\tilde{\boldsymbol{u}}(t) = \left[\begin{array}{cccc} k_{11}(t) & k_{12}(t) & k_{13}(t) & k_{14}(t) \\ k_{21}(t) & k_{22}(t) & k_{23}(t) & k_{24}(t) \end{array}\right]\left[\begin{array}{c} e_1(t) \\ e_2(t) \\ e_3(t) \\ e_4(t) \end{array}\right] \tag{28}$$

The controller is brought into the error time-varying system and the system matrix of the desired closed-loop system is set to

$$\boldsymbol{A}_{respect} = \begin{bmatrix} 0 & 1 & 0 & 0 \\ \lambda_1 & \lambda_2 & 0 & 0 \\ 0 & 0 & 0 & 1 \\ 0 & 0 & \lambda_3 & \lambda_4 \end{bmatrix} \tag{29}$$

Let the system matrix of the error time-varying system substituted into the closed-loop controller be equal to the expectation matrix, and the controller parameters can be solved.

$$\begin{cases} \begin{bmatrix} k_{11} \\ k_{21} \end{bmatrix} = \begin{bmatrix} b_{21} & b_{22} \\ b_{41} & b_{42} \end{bmatrix}^{-1} \begin{bmatrix} \lambda_1 \\ 0 \end{bmatrix} \\ \begin{bmatrix} k_{12} \\ k_{22} \end{bmatrix} = \begin{bmatrix} b_{21} & b_{22} \\ b_{41} & b_{42} \end{bmatrix}^{-1} \begin{bmatrix} \lambda_2 - a_{22} \\ -a_{24} \end{bmatrix} \\ \begin{bmatrix} k_{13} \\ k_{23} \end{bmatrix} = \begin{bmatrix} b_{21} & b_{22} \\ b_{41} & b_{42} \end{bmatrix}^{-1} \begin{bmatrix} -a_{23} \\ \lambda_3 - a_{43} \end{bmatrix} \\ \begin{bmatrix} k_{14} \\ k_{24} \end{bmatrix} = \begin{bmatrix} b_{21} & b_{22} \\ b_{41} & b_{42} \end{bmatrix}^{-1} \begin{bmatrix} 0 \\ \lambda_4 \end{bmatrix} \end{cases} \tag{30}$$

In [18-21], there is no description and explanation on how to select the controller parameters, and this paper will do the explanation after the above controller design. From the above derivation, we can see that the parameters of the controller are related to the expected characteristic roots, so the key problem of deciding the parameters lies in the selection of the expected characteristic roots, and the following characteristic equation of the expected closed-loop system matrix

$$\begin{cases} s^2 - \lambda_2(t)s - \lambda_1(t) = 0 \\ s^2 - \lambda_4(t)s - \lambda_3(t) = 0 \end{cases} \tag{31}$$

so that

$$\begin{aligned} \lambda_1(t) &= -\omega_1^2(t), \quad \lambda_2(t) = -2S_1(t)\omega_1^2(t) \\ \lambda_3(t) &= -\omega_2^2(t), \quad \lambda_4(t) = -2S_2(t)\omega_2^2(t) \end{aligned} \tag{32}$$

According to the current underdamped second-order linear system for the step response, the rise time and overshoot are estimated by equations

$$t_r = \frac{\pi - \arccos\,\zeta}{\omega\sqrt{1-\zeta^2}} \tag{33}$$

$$\sigma = \exp\left(\frac{-\pi\zeta}{\sqrt{1-\zeta^2}}\right) \times 100\% \tag{34}$$

Then the damping ratio and frequency of the desired system are solved jointly for the rise time and overshoot of the closed-loop control system given the demand, and then the characteristic roots of the desired system matrix are determined to obtain the controller parameters.

5. **Simulation Results of Parabolic Trajectory Profile Design and TLC Tracking.** In this section, for the parabolic pre-separation ascending trajectory scheme of RLV, the terminal flight speed $Ma_f = 6$, the terminal altitude $H_f = 27.8$ km, the terminal flight path angle $\theta_f = 0°$, the angle of attack shall not exceed 15° and shall not be less than −6°, with all these conditions and method which established in the previous section, simulation is carried out. And the results are shown in Figure 3.

From the figure, we can see that the pre-separation trajectory strategy design method proposed in this paper can satisfy the flight terminal condition.

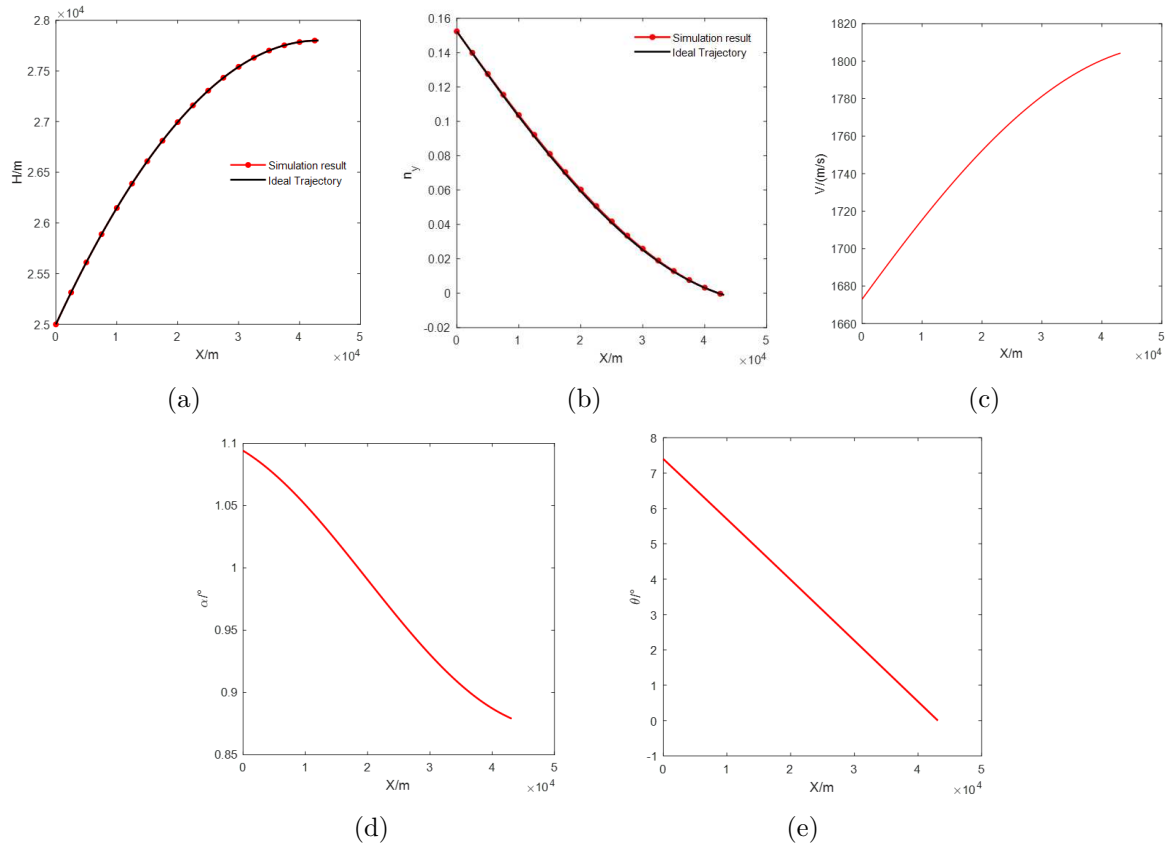

FIGURE 3. Simulation results of parabolic trajectory profile design: (a) Altitude result; (b) normal overload result; (c)-(e) profiles of speed, angle of attack, and flight path angle

The simulation results of the height profile and the normal overload profile show that the output error of the designed strategy is less than 0.5%. The output of velocity shows that the Mach number at the end of the trajectory can meet the constraint $Ma_f = 6$. The change of angle of attack in the whole flight profile is very small, which can be explained by the fact that the change of normal overload itself is not big, so the change of angle of attack, which mainly affects the lift performance of the aircraft, is not very big. The output of the flight path angle is related to the shape of the designed parabola. According to the description in Chapter 2, the course profile of the trajectory dip should be an even descent to zero; Figure 3(e) confirms this.

In Section 4, the tracking control law is carried out based on the TLC tracking control method. In order to check the tracking performance of the tracking controller, some of the aerodynamic properties of the RLV were subjected to certain positive and negative deviations during the simulation, as shown in Table 1.

TABLE 1. Aerodynamic properties deviations input for RLV

Variable	Description	Value
C_l	Lift coefficient of RLV	$\pm 10\%$
C_d	Drag coefficient of RLV	$\pm 10\%$
T	Thrust of RLV	$\pm 10\%$

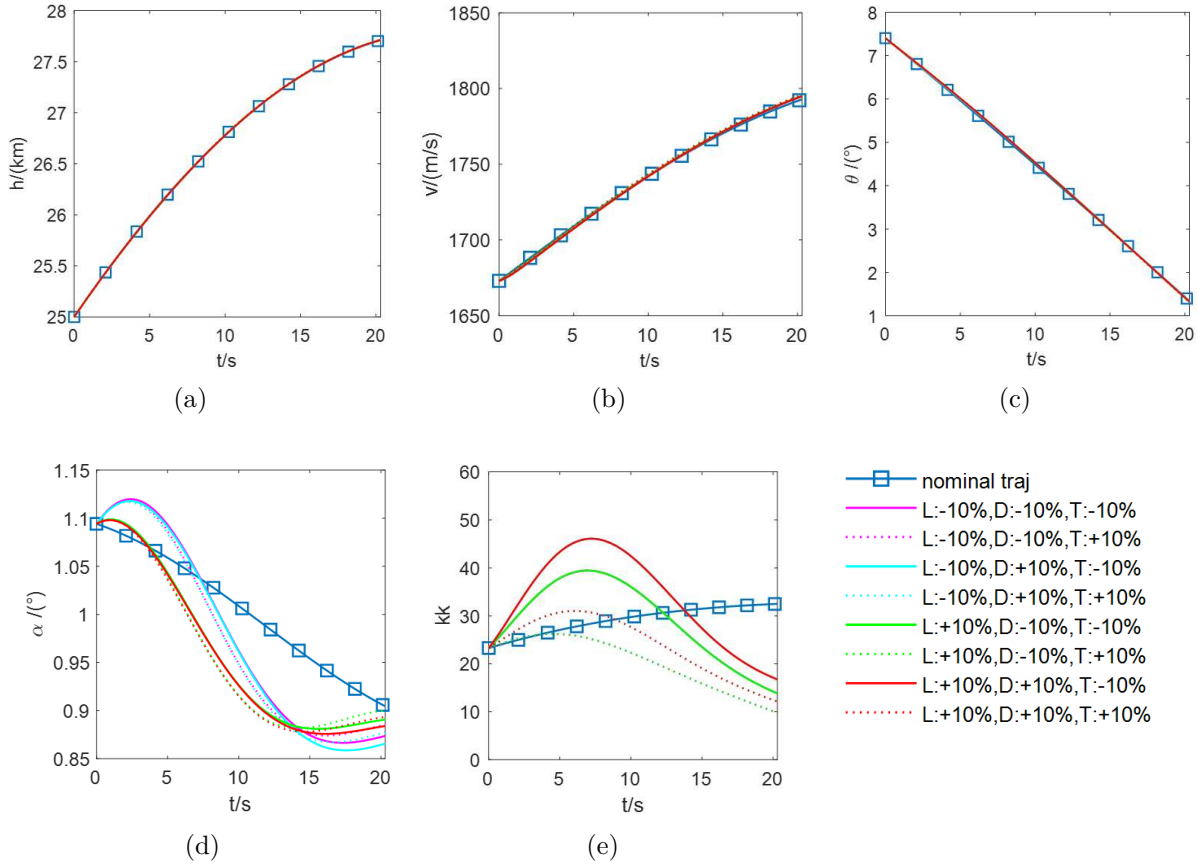

FIGURE 4. Simulation results of parabolic pre-separation trajectory tracking (L, T, D represent lift, thrust and drag): (a) Result of altitude; (b) result of speed; (c) result of flight path angle; (d) command of angle of attack; (e) command of throttle

From the simulation results shown in Figure 4, it can be seen as follows.

- The altitude and flight path angle are able to track the designed profile well.
- The maximum velocity tracking error is 4.65 m/s, which is within the controllable range, and the end velocities are able to meet the velocity requirements of the separation window.
- The command change of the angle of attack is generally seen to be related to the change of lift. When the lift coefficient decreases by 10%, the angle of attack must be increased in order to enable the vehicle to reach the original lift size, and when the lift coefficient increases by 10%, the angle of attack command decreases.
- The command change of the throttle, as a control input, needs to be actively changed to neutralize effects of the thrust and drag deviations.

From the simulation results of Figure 3 and Figure 4, it can be seen that the method proposed in this paper can solve the profile of the given parabola pre-separation trajectory and accomplish the guidance control of the trajectory successively, and the results show the accuracy of the section solution strategy, the accuracy of TLC tracking control and strong robustness. Although only one example of parabola trajectory is given in this paper, according to the derivation process of the algorithm formula, it is not difficult to see that the section solution algorithm designed in this paper can complete more section solutions of different shape trajectories, as long as the height-range profile of the section is mathematically continuous and smooth. Compared with the work of Sun et al. [12], the

method of this paper makes up for the shortcoming that the iterative algorithm cannot continue because of the singular value when the change rate of altitude of the trajectory with respect to range is zero.

6. **Conclusion.** In this work, a parabolic pre-separation trajectory strategy is carried out for the multi-body separation problem of TSTO RLV, considering the conditions required for successful separation. In the trajectory design segment, a profile design strategy based on the HDD is used to achieve the design function of inverse solving the flight profile for a known flight path shape.

Then a TLC method is used to design the tracking control law, and the controller parameters are also studied. And the nominal angle of attack and throttle commands are obtained from the trajectory tracking loop.

Finally, the simulation is verified by MATLAB, and deviations of several parameters are added to the simulation to check the performance of the controller. It is found that the controller is able to complete the designed profile well, and it also shows that the flight profile design strategy based on the HDD proposed in this work is feasible.

Overall, this paper has developed a pre-separation trajectory profile design tool, which provides a new technical approach to the orbiting of TSTO RLV.

REFERENCES

[1] L. Yang, Z. Ye and J. Wu, The influence of the elastic vibration of the carrier to the aerodynamics of the external store in air-launch-to-orbit process, *Acta Astronaut*, vol.128, pp.440-454, 2016.

[2] L. Yang and Z. Ye, The interference aerodynamics caused by the wing elasticity during store separation, *Acta Astronaut*, vol.121, pp.116-129, 2016.

[3] J. E. Bradford, A. Charania, J. Wallace et al., Quick-sat: A two-stage to orbit reusable launch vehicle utilizing air-breathing propulsion for responsive space access, *Space 2004 Conference and Exhibit*, San Diego, CA, DOI: 10.2514/6.2004-5950, 2004.

[4] T. Kokan, J. R. Olds, V. Hutchinson et al., *Aztec*: A TSTO hypersonic vehicle concept utilizing TBCC and HEDM propulsion technologies, *The 40th AIAA/ASME/SAE/ASEE Joint Propulsion Conference and Exhibit*, Fort Lauderdale, FL, 2004.

[5] N. Mcnelis and P. Bartolotta, Revolutionary turbine accelerator (RTA) demonstrator, *AIAA/CIRA 13th International Space Planes and Hyper-Sonics Systems and Technologies*, 2005.

[6] K. Bowcutt, M. Gonda, S. Hollowell et al., Performance, operational and economic drivers of reusable launch vehicles, *Indianapolis: The 38th AIAA/ASME/SAE/ASEE Joint Propulsion Conference & Exhibit*, 2002.

[7] M. Bradley, K. Bowcutt and J. Mccomb, Revolutionary turbine accelerator (RTA) two-stage-to-orbit (TSTO) vehicle study, *Indianapolis: The 38th AIAA/ASME/SAE/ASEE Joint Propulsion Conference & Exhibit*, 2002.

[8] W. She, X. Liu and K. Liu, Analysis and thinking on technical approach of Sanger aerospace vehicle, *Journal of Rocket Proplusion*, vol.47, no.6, pp.11-20, 2021.

[9] D. J. Dalle, S. M. Torrez and J. F. Driscoll, Minimum-fuel ascent of a hypersonic vehicle using surrogate optimizatio, *Journal of Aircraft*, vol.51, no.6, pp.1973-1986, 2014.

[10] S. Keshmiri, R. Coleren and M. Mirmirani, Six-DOF modeling and simulation of a generic hypersonic vehicle for control and navigation purposes, *AIAA Guidance, Navigation, and Control Conference*, 2006.

[11] T. Peng, L. Meng and Y. Ye, Guidance technology for autolanding of unpowered reusable launch vehicle, *Journal of Terahertz Science and Electronic Information Technology*, vol.12, no.2, pp.208-212+228, 2014.

[12] P. Sun, Y. Liu and B. Chen, Ascent trajectory design of hypersonic vehicle based on preset dynamic pressure, *Flight Dynamics*, vol.35, no.5, pp.57-61, 2017.

[13] T. Chao, Y. Wang, S. Wang et al., Trajectory tracking control for non-minimum phase hypersonic vehicles, *Systems Engineering and Electronics*, vol.466, no.40, pp.137-142, 2018.

[14] P. Zhang, L. Liu and J. Wang, Optimal ascent trajectory design for single-stage-to-orbit space planes based on Gauss pseudospectral method, *Aerospace Control and Application*, vol.43, no.2, pp.13-20, 2017.

[15] N. Kumyaito and K. Tamee, Trajectory clustering by GPS tracking dataset using QuickBundles, *ICIC Express Letters, Part B: Applications*, vol.11, no.10, pp.921-928, 2020.
[16] Z. Luo, S. Wang, X. Yan and X. Li, Trajectory optimization design of ascending stage of RBCC powered hypersonic vehicle, *Infrared and Laser Engineering*, vol.51, no.8, DOI: 10.3788/IRLA20210956, 2022.
[17] C. He, X. Chen and L. Wu, Research of guidance and control technologies for reusable launch vehicle sub-orbital ascent flight, *Journal of Applied Sciences*, vol.28, no.2, pp.216-220, 2010.
[18] Z. Zhang, Reusable space vehicle flight control, *Journal of Beijing University of Aeronautics and Astronautics*, vol.29, no.12, pp.1-5, 2003.
[19] K. Liu, J. Guo and W. Zhou, Investigation on ascent guidance law for air-breathing combined-cycle hypersonic vehicle, *Journal of Astronautics*, vol.41, no.8, pp.1023-1031, 2020.
[20] M. Mickle and J. Zhu, Bank-to-tum roll-yaw-pitch autopilot design using dynamic nonlinear inversion and PD-eigenvalue assignment, *The 26th American Control Conference*, Chicago, USA, 2000.
[21] M. Mickle and J. Zhu, Skid-to-tum control of the apkws missile using trajectory linearization technique, *The 27th American Control Conference*, Arlington, USA, 2001.
[22] X. Wu, Y. Liu and J. Zhu, Design and real time testing of a trajectory linearization flight controller for the "Quanser UFO", *The 29th American Control Conference*, Denver, USA, pp.3913-3918, 2003.

Author Biography

Honglin Liu received B.S. in Dalian University of Technology in 2021. He is currently studying for M.S. in Aerospace Science and Technology at Dalian University of Technology. His research interests include flight guidance and control.

Rui Wang received her B.Sc. and M.Sc. in Mathematics from Bohai University, China, in 2001 and 2004, respectively, and her Ph.D. in Control Theory and Applications from Northeastern University, China, in 2007. From March 2007 to December 2008, she was a visiting research fellow at the University of Glamorgan, Pontypridd, UK. She is currently a professor at the School of Aeronautics and Astronautics, Dalian University of Technology, China. Her main research interests include switched systems, robust control, and aero-engine control.

Weiguang Shao received B.S. in Dalian University of Technology in 2021. He is currently studying for M.S. in Aerospace Science and Technology at Dalian University of Technology. His research interests include pneumatic servoelasticity and sensor fusion algorithms.

Kai Liu received the B.S. degree in Information and Computing Science from Jilin University, China, 2007. And he received the Ph.D. from Harbin Institute of Technology, China, 2013. He is currently an associate professor at Dalian University of Technology. His research interests include flight guidance and control.